Silicon Photonics
矽光子學
A Selection of Photonic Devices (B)

課程編號：941 U0460
科目名稱：矽光子學
授課教師：黃鼎偉
時間地點：一678 明達館 303

Outline

- 6.1 OPTICAL PHASE MODULATORS AND VARIABLE OPTICAL ATTENUATORS (continued)
- 6.2 THE MACH-ZEHNDER INTERFEROMETER
- 6.3 THE WAVEGUIDE BEND

6.1 OPTICAL PHASE MODULATORS AND VARIABLE OPTICAL ATTENUATORS (continued)

Predicted Device Operation as a Phase Modulator

- Based upon the modeling in the preceding sections we can define a device to produce the best performance, based upon the parameters investigated.
- The device should have sloping rib walls, and a rib height of 3.2 μm (although it would be reasonable to trade this off for simpler fabrication).
- The n^+ doping contacts should be close to the base of the rib, and a contact depth of the order of 1.2 μm (although once again it would be reasonable to trade this off against ease of fabrication and avoidance of additional absorption).

Predicted Device Operation as a Phase Modulator

- Such a device delivers an approximately uniform injected carrier density of 2.2 x 10^{17} cm^{-3}, at a forward bias of 0.9V.
- Assuming a wavelength of operation of 1.55 μm, and using equation 4.64, we can evaluate the predicted change in refractive index in the guiding region, Δn, as:

$$\begin{aligned}\Delta n &= \Delta n_e + \Delta n_h = -[8.8 \times 10^{-22}\Delta N_e + 8.5 \times 10^{-18}(\Delta N_h)^{0.8}] \\ &= -[8.8 \times 10^{-22}(2.2 \times 10^{17}) + 8.5 \times 10^{-18}(2.2 \times 10^{17})^{0.8}] \\ &= -8.3 \times 10^{-4} \end{aligned} \quad (6.1)$$

Predicted Device Operation as a Phase Modulator

- The refractive index change results in a phase change of the propagating optical mode, $\Delta\varphi$ given approximately by:

$$\Delta\phi = \frac{2\pi\Delta nL}{\lambda_0}$$

where *L* is the length of the active region of the modulator.

- A useful benchmark in comparing optical modulators based upon carrier injection is the current required to produce an optical phase shift of π radians for a unit length of the modulator.

Predicted Device Operation as a Phase Modulator

- In this example we can use the concept of a π-radian phase shift to determine the length required to produce such a phase shift, for a fixed level of injection.
- Therefore using equation 6.2, and setting $\Delta\varphi = -\pi$, the required length is:

$$L_\pi = \frac{\lambda_0}{2\Delta n} = 934\,\mu m$$

- This is not an unreasonable length for such a device, but is perhaps getting a little long.
- Consequently the device could be improved by increasing the doping density in the contact regions, which would in turn allow more efficient carrier injection, or simply driven a little harder (i.e. more forward bias), to inject more charge per unit length, and hence obtain more phase change per unit length.

Associated Absorption of the Phase Modulator

- We can also predict the additional absorption loss of the same device when forward-biased at 0.9 V.
- Using equation 4.65, the additional loss,

$$\begin{aligned}\Delta\alpha &= \Delta\alpha_e + \Delta\alpha_h = 8.5 \times 10^{-18}\Delta N_e + 6.0 \times 10^{-18}\Delta N_h \\ &= 8.5 \times 10^{-18}(2.2 \times 10^{17}) + 6.0 \times 10^{-18}(2.2 \times 10^{17}) \\ &= 3.19\,cm^{-1} \end{aligned} \quad (6.4)$$

- This is equivalent to an enormous 13.9 dB/cm, but since the device is only 934 μm, the additional loss would be 1.3 dB.

Associated Absorption of the Phase Modulator

- Because this device discussed in the previous section was a phase modulator, the intention was to minimize the absorption loss (attenuation).
- However, if we wanted to produce a variable optical attenuator (VOA) we could make the device longer to maximize the attenuation, and also drive the device to a higher potential increasing the level of injected charge.

Associated Absorption of the Phase Modulator

- For example if we drive the device harder to produce a level of injection of 5 x 10^{18}, the attenuation becomes:

$$\begin{aligned}\Delta\alpha &= \Delta\alpha_e + \Delta\alpha_h = 8.5\times10^{-18}\Delta N_e + 6.0\times10^{-18}\Delta N_h \\ &= 8.5\times10^{-18}(5\times10^{18}) + 6.0\times10^{-18}(5\times10^{18}) \\ &= 72.5\,\text{cm}^{-1} \end{aligned} \quad (6.5)$$

- This is equivalent to 315 dB/cm, equivalent to 29.4 dB for a device 934 μm in length, or 63 dB for a 2-mm long device.
- Clearly this is an enormous attenuation, and very useful as a variable optical attenuator, because the attenuation available covers a very large dynamic range.

Fabrication and Experimental Results

- A device similar to that described in the previous section was reported by Tang and Reed [2] in 1995.
- Due to fabrication tolerances, the devices fabricated had different dimensions than those modeled.
- Therefore, for the purposes of this text it is instructive to consider a device of considerably different dimensions to demonstrate how to compare differing devices.
- Consider the device shown in Figure 6.14, which was one of the devices fabricated.
- The device was fabricated with the cross-sectional characteristics shown in the figure, and an active length of 500 μm.

Fabrication and Experimental Results

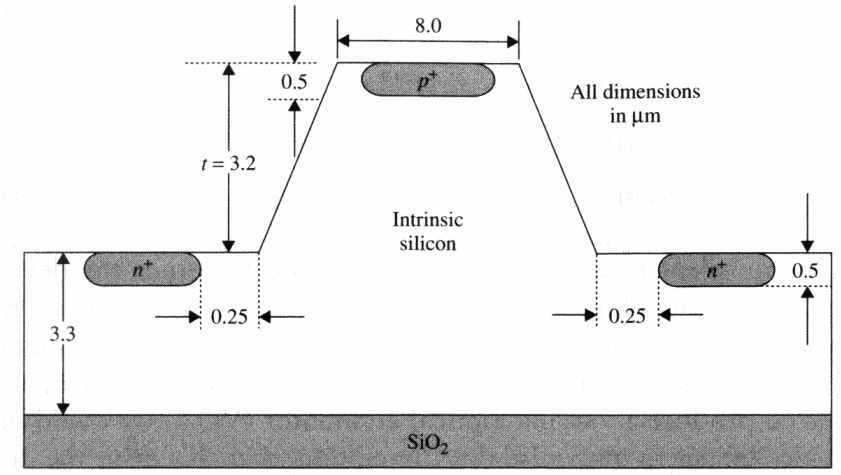

Figure 6.14 Experimental phase modulator.

Fabrication and Experimental Results

- Note that according to the single-mode criteria of Soref, this device may not be a single-mode device. However, experimentally only a single mode was observed, suggesting higher-order modes were sufficiently lossy that they were insignificant.
- A phase modulator is often fabricated as part of an interferometer, so the modulator causes a phase change in one arm of the interferometer, with reference to the static phase in the second arm of the interferometer (for example, a Mach-Zehnder interferometer, the operation of which is discussed later in this chapter).

Fabrication and Experimental Results

- An integrated Mach-Zehnder interferometer is shown in Figure 6.15.

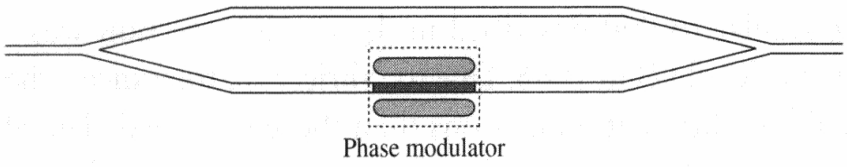

Figure 6.15 Schematic of a Mach-Zehnder interferometer containing a phase modulator

Fabrication and Experimental Results

- However, integrating the device with other components introduces the additional losses associated with the other components, and in this case it was desirable to measure the characteristics of the phase modulator in isolation, such as the passive and active loss of the waveguide.
- Therefore the device was fabricated as part of a straight waveguide.
- This means that measurement of phase is more difficult, and must be carried out as part of a free-space interferometer.
- Such a system is shown in Figure 6.16.

Fabrication and Experimental Results

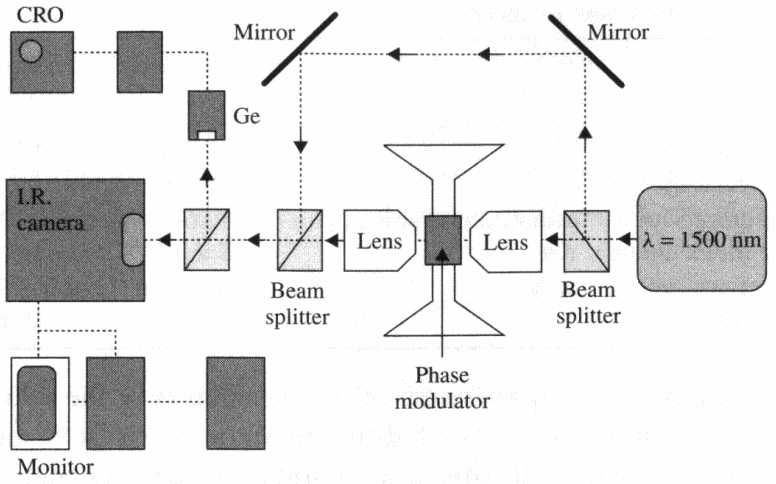

Figure 6.16 Free-space configuration of a Mach-Zehnder interferometer.

Fabrication and Experimental Results

- In the integrated Mach-Zehnder interferometer, interference occurs when the two arms of the interferometer are recombined.
- The resultant intensity manifests itself as the intensity of the mode in the output waveguide, as discussed later in this chapter.
- In the free-space interferometer, the two beams from separate paths interfere on a screen (camera in this case), and interference fringes are observed, because the interference is not constrained within the waveguide, and perfect overlay of the two beams is unlikely.
- Therefore it is a simple matter to measure π-radian phase shift in the integrated interferometer, because this corresponds to the shift from maximum intensity to minimum intensity. In the free-space interferometer, it is necessary to monitor the movement of the interference fringes by half of one period.
- This can be done using video capture techniques.

Fabrication and Experimental Results

- The experimental devices were measured as described above, and the following results are representative of the devices measured:
  - Current required for a π-radian phase shift (I_π): 7 mA
  - Passive waveguide propagation loss (modulator off): 0.7 dB/cm
  - Additional active optical loss (modulator biased to I_π): 1.3 dB.
- Whilst the device has different dimensions than the modeled device, it is possible to make comparisons by considering the current density of each device.
- The modeled device had a rib width of 4 μm, and a length 934 μm, together with I_π = 4.03 mA.

Fabrication and Experimental Results

- Since this current flows through the rib surface, the current density, *J*, at this point is:

$$J_M = \frac{4.03 \times 10^{-3}}{(4 \times 10^{-4})(934 \times 10^{-4})} = 108\ \text{A/cm}^2$$

- Similarly for the experimental device:

$$J_E = \frac{7 \times 10^{-3}}{(8 \times 10^{-4})(500 \times 10^{-4})} = 175\ \text{A/cm}^2$$

- Since the devices are of different lengths, obviously the current densities are different.

Fabrication and Experimental Results

- One way to compare devices of different dimensions is to normalize via a figure of merit, χ. In this case, a suitable figure of merit may be defined as:

$$\chi = \frac{\phi}{JL}$$

- where χ is phase shift in degrees, *J* is current density, and *L* is the device length. The figure of merit is included in the comparison Table 6.2.

Table 6.2 A comparison of theoretical and experimental performance

Parameter	Modelled device	Experimental device
Current density, J	108 A/cm^2	175 A/cm^2
Active optical loss	1.3 dB	1.3 dB
Current required for a π-radian phase shift, I_π	4 mA	7 mA
Refractive index change, Δn	-8.3×10^{-4}	-1.55×10^{-3}
Peak carrier concentration, N	2.2×10^{17} cm^{-3}	4.6×10^{17} cm^{-3}
Figure of merit, χ	17.8°cm/A	20.6°cm/A

Fabrication and Experimental Results

- We can see from Table 6.2 that, despite the differences between the two modulator dimensions, the figure of merit is in reasonable agreement, and is a direct consequence of optimization via the modeling.
- This statement has more impact when it is pointed out that, at the time these devices were fabricated, the typical current densities being reported in the literature for carrier injection devices were of the order of kA/cm^2.
- Therefore this device represented an improvement in the state of the art of approximately an order of magnitude.

Influence of the Thermo-optic Effect on Experimental Devices

- Having fabricated a carrier Injection device in silicon, the possibility exists that the thermo-optic effect may diminish the efficiency with which the device operates.
- It is possible to estimate the worst-case effect of the thermo-optic effect very simply.
- This can be done by adopting a simple one-dimensional model of heat transfer to our device, and assuming that all of the power used to operate the device contributes to heating.
- In effect this means we are assuming that there is no heat loss from conduction, convection or radiation.

Influence of the Thermo-optic Effect on Experimental Devices

- This is clearly not the case, but it enables us to calculate the absolute worst-case contribution of the thermo-optic effect.
- Heat transfer to the device is then given by

$$P = \frac{\Delta T w L}{(t_{si}/k_{si})}$$

where P is the applied power, ΔT is the temperature rise, w is device width, L is device length, t_{si} is the device thickness (silicon layer), and k_{si} is the thermal conductivity of silicon.

- For the experimental device reported in the previous section, the applied power (at I_π) was 11.9 mW.

Influence of the Thermo-optic Effect on Experimental Devices

- Since the thermal conductivity of silicon at room temperature is k_{si} = 1.56 W/cm/K, then for an applied power of 11.9 mW the temperature rise ΔT is:

$$\Delta T = \frac{P(t_{si}/k_{si})}{wL} = 0.124\,\mathrm{K}$$

- We know from equation 4.69 that the corresponding rise in refractive index will be given by:

$$\frac{dn}{dT} = 1.86 \times 10^{-4}/\mathrm{K}$$

so, $$\Delta n = 1.86 \times 10^{-4}(0.124) = 2.3 \times 10^{-5}$$

Influence of the Thermo-optic Effect on Experimental Devices

- Therefore, even in the worst-case situation where all power contributes to the thermo-optic effect, the change in refractive index due to this effect is very small.
- In order to compare the two effects, we can evaluate the ratio of the refractive index changes:

$$\left|\frac{\Delta n_{\text{fc}}}{\Delta n_{\text{toe}}}\right| = \frac{1.55 \times 10^{-3}}{2.3 \times 10^{-5}} = 67.4$$

Influence of the Thermo-optic Effect on Experimental Devices

- That is, the change in refractive index due to the injection of free carriers is 67.4 times larger than that due to the thermo-optic effect.
- Of course, in reality the ratio will be even larger, as some of the heat will be lost by conduction, convection and radiation.
- Hence we can conclude that the influence of the thermo-optic effect is negligible in this case.
- Had the influence not been negligible it would have been worth evaluating the heating effect more accurately.

Switching Characteristics of the Optical Phase Modulator

- The details of the optical phase modulator discussed thus far have all considered the DC performance of the device.
- However, of paramount importance is also the switching characteristic of such a device, because the phase modulator could form part of an intensity modulator, or indeed an optical switch if configured as part of some form of interferometer as discussed above.
- The switching time then determines the speed of the device, and therefore the range of application for which it is useful.

Switching Characteristics of the Optical Phase Modulator

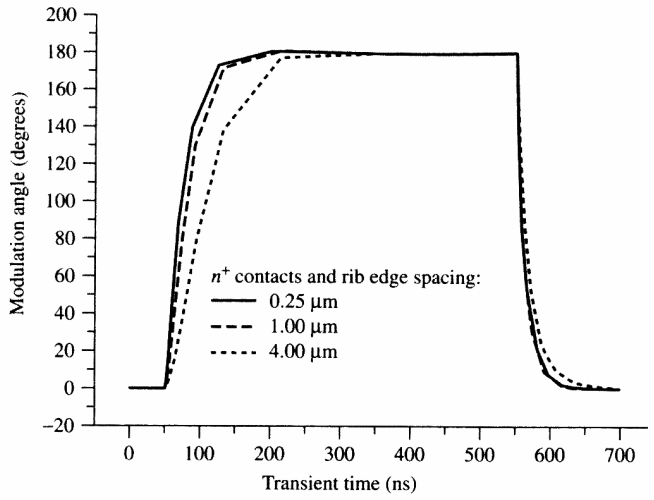

Figure 6.17 Modeled rise and fall times of the optical phase modulator

Switching Characteristics of the Optical Phase Modulator

- One of the most convenient ways of determining the switching speed (or time) of the optical phase modulator is to drive it with a fast square wave, and record the rise time of the resulting phase change.
- We can then characterize the device in terms of its rise and fall times.
- Figure 6.17 shows the modeled response of the modulator in Figure 6.7, but for the three positions of the n^+ contacts.
- The three positions are those used for the DC calculations earlier when we were comparing injection efficiency of the carriers (Figure 6.13).

Switching Characteristics of the Optical Phase Modulator

- Therefore the distances from the base of the rib to the n^+ contact region of 0.25 μm, 1 μm and 4 μm were used for the simulation.
- For these transient solutions, the device anode and cathode were first zero-biased for 50 ns, followed by a step increase to V_π for 500ns, and finally a step decrease to 0V.
- In each case, V_π is the voltage corresponding to a 180º phase shift.
- The rise time, t_r is defined as the time required for the induced phase shift to change from 10 % to 90 % of the maximum value, and the fall time t_f is defined as the time required for the induced phase shift to change from 90 % to 10 % of the maximum value.

Switching Characteristics of the Optical Phase Modulator

- We can see from Figure 6.17 that the rise time is significantly slower than the fall time of this device, and is therefore the limiting transition.
- More importantly we see that the rise time for the device with contacts far from the rib is significantly slower than the device with contacts close to the rib.
- This is primarily a consequence of the additional time taken for the charges to be moved through a greater distance, and as such is not surprising (although there are also secondary effects that change the rise time).

Switching Characteristics of the Optical Phase Modulator

- The rise time for the fastest device (0.25 μm spacing) is 58.3 ns, and the fall time is 33.1 ns, corresponding to a bandwidth of the order of 6 MHz.
- The device with the 1 μm spacing has a rise time of 65.5 ns and a fall time of 31.4 ns, and the device with the 4 μm spacing has a rise time of 117 ns and a fall time of 43.5 ns.
- This clearly demonstrates the effect on the response time due to changing the device dimensions.
- Even the fastest of the three devices is a relatively slow device, and certainly not sufficiently fast for optical communications.

Switching Characteristics of the Optical Phase Modulator

- The device is limited by the fact that switching requires the movement of a significant amount of charge over a fixed distance.
- Making the device smaller will immediately improve the response time of the devices, because the time taken to move the charge will be reduced.
- Recent work by Png et al. has shown that silicon devices with bandwidths in excess of 1 GHz are predicted.
- Given the relatively preliminary nature of this work it is probable that much faster silicon devices will emerge in the future.

6.2 THE MACH-ZEHNDER INTERFEROMETER

THE MACH-ZEHNDER INTERFEROMETER

- Interferometers are central to many optical circuits, but one of the most frequently used interferometers is the famous Mach-Zehnder type.
- The device is shown schematically in Figure 6.18.
- The Mach-Zehnder interferometer is a common device in optical circuits, being the basis of several other devices such as modulators, switches and filters.
- Let us briefly review the operation of the interferometer.
- Firstly consider an input wave, at the input waveguide, and let the wave be of TE polarization.

THE MACH-ZEHNDER INTERFEROMETER

- Assuming the waveguide splitter (Y-junction) at the input of the interferometer divides the wave evenly, the intensities in arm 1 and arm 2 of the interferometer will be the same.
- We can represent the electric fields of the propagating modes in arm 1 and arm 2 of the interferometer as E_1 and E_2 respectively, where:

$$E_1 = E_0 \sin(\omega t - \beta_1 z)$$

$$E_2 = E_0 \sin(\omega t - \beta_2 z)$$

- Consider that the two fields to have the same amplitude, but different propagation constants.

THE MACH-ZEHNDER INTERFEROMETER

- The two fields propagate along their respective arms of the interferometer and recombine at the output waveguide.
- When the input Y-junction divides the input field, the two fields formed in arm 1 and arm 2 will be in phase.
- However, when the fields recombine, they may no longer be in phase, either due to different propagation constants in the arms, or due to different optical path lengths in the arms.

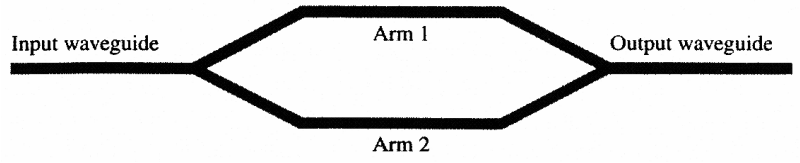

Figure 6.18 Schematic of a waveguide Mach-Zehnder interferometer

THE MACH-ZEHNDER INTERFEROMETER

- The intensity at the output waveguide, S_T, will be:

$$S_{\mathrm{T}} = [(E_1 + E_2) \times (H_1 + H_2)] = S_0(E_1 + E_2)^2$$

- Therefore we need to evaluate the term $(E_1+E_2)^2$.
- Let us assume different path lengths for the two waves, of L_1 and L_2
- Expanding and substituting for E_1 and E_2 gives:

$$S_{\mathrm{T}} = S_0\{E_0^2 \sin^2(\omega t - \beta_1 L_1) + E_0^2 \sin^2(\omega t - \beta_2 L_2) + 2E_0^2 \sin(\omega t - \beta_1 L_1) \sin(\omega t - \beta_2 L_2)\}$$

THE MACH-ZEHNDER INTERFEROMETER

- Using trigonometric identities, equation 6.16 can be

$$S_{\mathrm{T}} = S_0\{E_0^2(\tfrac{1}{2}[1 - \cos(2\omega t - 2\beta_1 L_1)]) + E_0^2(\tfrac{1}{2}[1 - \cos(2\omega t - 2\beta_2 L_2)]) + E_0^2[\cos(\beta_2 L_2 - \beta_1 L_1) - \cos(2\omega t - \beta_2 L_2 - \beta_1 L_1)]\} \quad (6.17)$$

- Since optical frequencies are very high, only the time average of these waves can be observed.
- Hence all terms in equation 6.17 must be replaced with their time average equivalent, yielding equation 6.18:

$$S_{\mathrm{T}} = S_0\left\{\frac{E_0^2}{2} + \frac{E_0^2}{2} + E_0^2[\cos(\beta_2 L_2 - \beta_1 L_1)]\right\} = S_0\{E_0^2[1 + \cos(\beta_2 L_2 - \beta_1 L_1)]\}$$

THE MACH-ZEHNDER INTERFEROMETER

- Equation 6.18 is the well-known transfer function of the interferometer, which is plotted in Figure 6.19, normalized to a maximum amplitude of 1.
- The term ($\beta_2 L_2$ - $\beta_1 L_1$) represents the phase difference between the waves from each arm of the interferometer.
- Clearly if the two arms of the interferometer have identical waveguides, and hence identical propagation constants, the transfer function will have maxima when the path length difference, $|L_2 - L_1|$, results in a phase difference of a multiple of 2π radians.
- Similarly the transfer function will have minima when the phase difference is a multiple of π radians.

THE MACH-ZEHNDER INTERFEROMETER

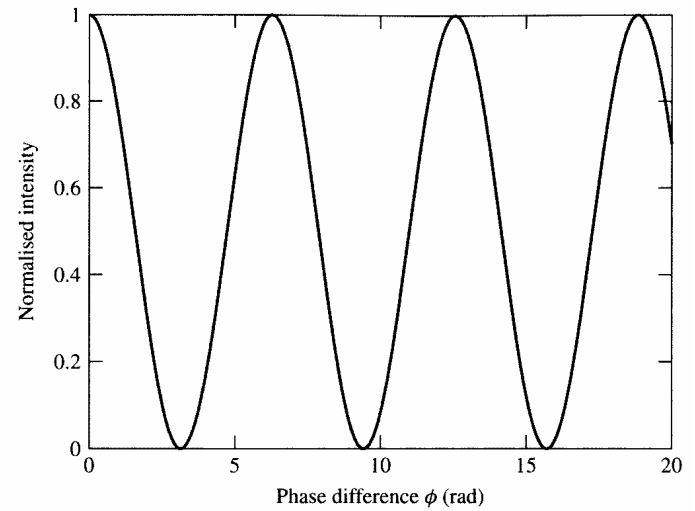

Figure 6.19 Normalized transfer function of a Mach-Zehnder interferometer

THE MACH-ZEHNDER INTERFEROMETER

- Thus the intensity at the output of the Mach-Zehnder interferometer can be manipulated to be a maximum or a minimum, by varying the relative phase of the two arms of the interferometer.
- This could be accomplished by inserting an optical phase modulator into one of the interferometer arms.
- In the case of the silicon modulator discussed in the previous section, the unwanted additional absorption due to free carriers will result in an imbalance in the intensities in each of the interferometer arms, and consequently, in imperfect interference in the output waveguide, and in particular in an imperfect 'null' in the transfer function.
- If such an intensity modulator is to be used over less than 2π radians, one arm can be biased in terms of loss, to compensate.

6.3 THE WAVEGUIDE BEND

WAVEGUIDE BEND

- The majority of the waveguides discussed so far in this text have been depicted as simple straight structures, uniform in the *z* direction (except for the waveguides forming the Mach-Zehnder interferometer).
- However, to make the optical circuits practical we need to be able to send light to various parts of the circuit. This means that we must be able to form bends in the waveguide.
- Alternatively, one could imagine a series of straight waveguides joined together, but the abrupt junction of such waveguides would result in scattering centers, and hence losses would result at each abrupt change.
- A curved waveguide allows a gradual transition from one direction to another that can have negligible loss.

WAVEGUIDE BEND

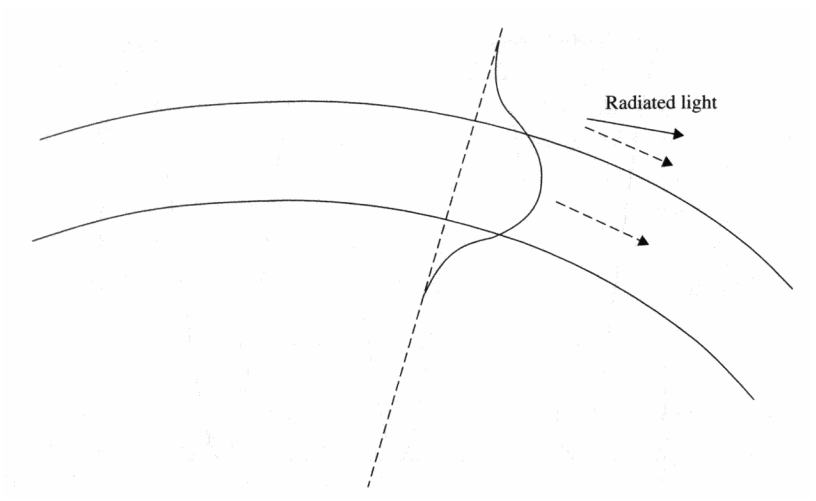

Figure 6.20 Radiation loss from an optical fiber bend.

WAVEGUIDE BEND

- At first sight, it may seem extravagant to regard a simple curve in a waveguide as a separate device, and hence perhaps it is unexpected to find bends covered in this chapter.
- However, like many other optical devices, the bend requires careful design in order that it is not lossy.
- For this reason it is included in this chapter, so that we can use the knowledge we have gained in earlier chapters to understand the design issues for the waveguide bend.
- Consider Figure 6.20, which shows an optical fiber bend top view.
- An illustration of the lateral optical field is also shown, including the evanescent fields that extend into the cladding.
- It is convenient to consider the optical fiber, as the symmetrical nature of the fiber simplifies the explanation of loss.
- We will consider a rib waveguide subsequently.

WAVEGUIDE BEND

- Consider the mode shown in Figure 6.20, traveling around the fiber bend.
- Because the arc of the bend at the outside of the bend is longer than the arc at the inside of the bend, light at the outer cladding must propagate more quickly than light at the inner cladding, in order to maintain the phase relationship across the mode.
- As the evanescent tail extends into the outer cladding, eventually a distance is reached where light in the outer cladding will need to exceed the velocity of unguided light in the same material, in order to maintain the mode.
- This is, of course, impossible, so light is radiated and lost from the mode.

WAVEGUIDE BEND

- A similar situation occurs in a waveguide mode, although the geometrical shape of the waveguide is more complex.
- Such a situation is shown in Figure 6.21.

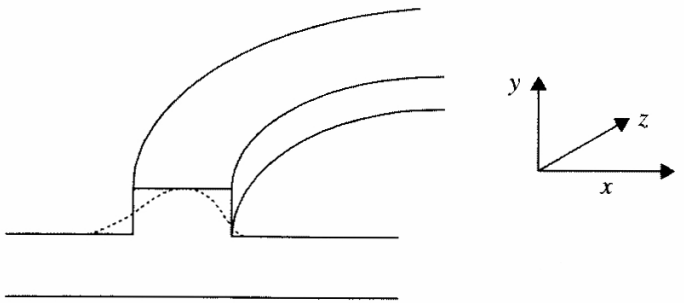

Figure 6.21 Waveguide bend showing distorted lateral mode shape.

WAVEGUIDE BEND

- Marcatili and Miller [9] carried out an analysis of such a waveguide bend to determine the loss coefficient.
- Whilst their analysis was not for a rib waveguide, the use of appropriately calculated propagation constants and decay constants inside and outside the rib gives reasonable results for a rib waveguide.
- They used an assumption that waveguide radiation from a bend was similar to emission of photons from an abruptly ended waveguide.
- This enabled them to determine a criteria for defining when light was lost from the guide, and hence define a distance from the side of the bend when light could be considered sufficiently far to no longer be part of the propagating mode.

WAVEGUIDE BEND

- This is a consequence of having to consider the distortion of the mode traveling around a bend, as shown in Figure 6.21, and to decide when light is sufficiently far from the waveguide to be considered lost.
- However, their analysis was based upon modes defined within the straight waveguide.
- Nonetheless, their result is widely used, partly due to the mathematical convenience.
- They showed that the loss coefficient from the bend was of the form:

$$\alpha_{\text{bend}} = C_1 \exp(-C_2 R) \qquad (6.19)$$

- where R is the bend radius, and C_1 and C_2 are related to the waveguide and mode properties.

WAVEGUIDE BEND

- The constants C_1 and C_2 are given by:

$$C_1 = \frac{\lambda_0 \cos^2\left(k_{xg}\frac{w}{2}\right)\exp(k_{xs}w)}{w^2 k_{xs} n_{effp}\left[\frac{w}{2} + \frac{1}{2k_{xg}}\sin(wk_{xg}) + \frac{1}{k_{xs}}\cos^2\left(k_{xg}\frac{w}{2}\right)\right]}$$

$$C_2 = 2k_{xs}\left(\frac{\lambda_0 \beta}{2\pi n_{effp}} - 1\right)$$

where β is the z-directed propagation constant, k_{xg} is the x-directed propagation constant in the waveguide, k_{xs} is the x-directed decay constant representing the evanescent field, w is the waveguide width, n_{effp} is the effective index outside the rib, and λ_0 is the free-space wavelength.

WAVEGUIDE BEND

- Consider the rib waveguide of Figure 6.22.
- Firstly let us consider a waveguide with the following parameters: h = 5 μm, r = 3 μm and w = 3.5 μm.
- For these conditions, and assuming TE polarization at a wavelength of λ = 1.55 μm, we can evaluate the bend radius from equation 6.19, for a bend loss of 0.1 dB/cm.
- The resulting bend radius is approximately 7.3 mm, rather large.
- It is worth noting that this figure agrees reasonably well with the sort of figures achieved experimentally, giving some confidence in the model.
- However, it should also be remembered that this is a simple model of a waveguide bend, and so is rather approximate.

WAVEGUIDE BEND

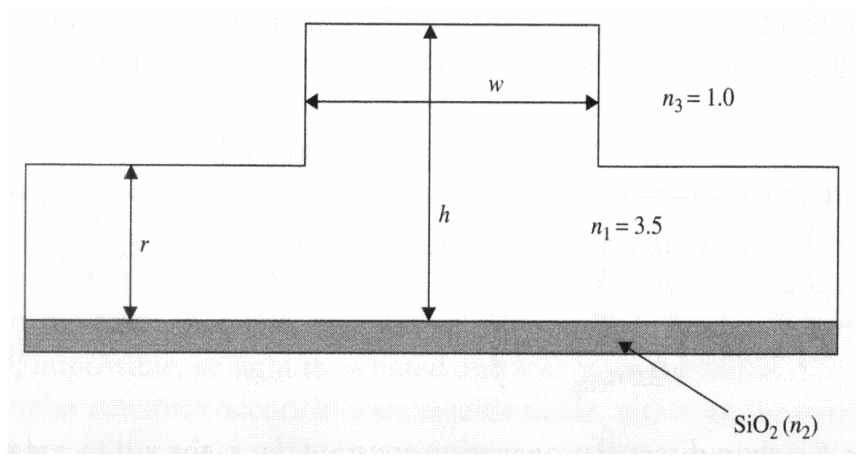

Figure 6.22 Rib waveguide geometry

WAVEGUIDE BEND

- It is helpful to consider the variation of bend loss with radius of the bend.

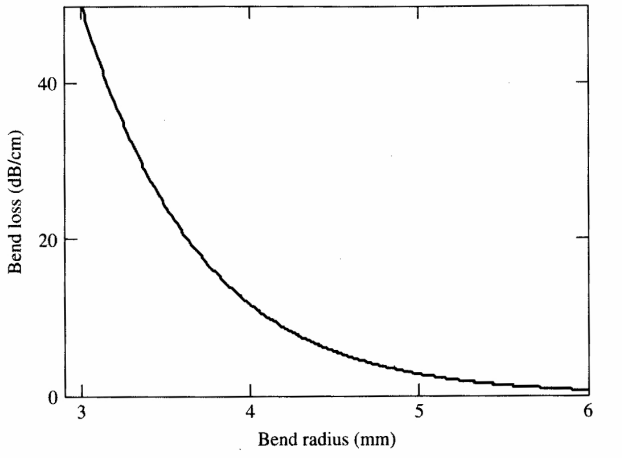

Figure 6.23 Bend loss variation with bend radius for a large rib waveguide

WAVEGUIDE BEND

- Before moving to a smaller waveguide, it is interesting to consider the effect of etching the waveguide a little more deeply, and hence better confining the mode.
- Let the conditions now be: h = 5 μm, r = 2.5 μm and w = 3.5 μm.
- Therefore the waveguide sidewalls have been etched by a further half of one micrometer.
- The radius of a waveguide with a loss of 0.1 dB/cm now falls to only 3.0 mm, significantly smaller.

WAVEGUIDE BEND

- Let us now consider a much smaller waveguide.
- Let the waveguide parameters be: h = 2 μm, r = 1.2μm and w = 1.4 μm.
- Proportionally these are the same dimensions as for the large rib discussed above.
- However, the bend radius of a waveguide with a loss of 0.1 dB/cm now falls to 0.74 mm.
- We can plot the variation in loss as a function of bend radius, as we did for a larger rib, shown in Figure 6.24.

WAVEGUIDE BEND

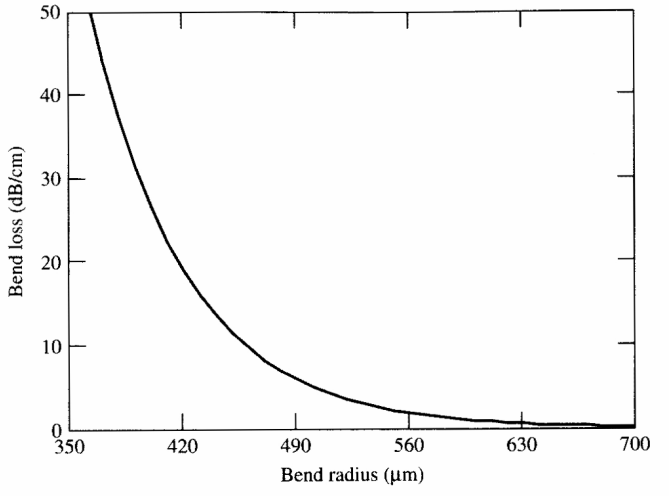

Figure 6.24 Bend loss variation with bend radius for a small rib waveguide

WAVEGUIDE BEND

- In a similar fashion to the previous example, let us now etch a little deeper into a small waveguide, so that the parameters become: h = 2 μm, r = 1.0 μm and w = 1.4 μm.
- In this case the waveguide now can tolerate a bend radius of only 310 microns.
- Clearly the smaller the waveguides become, the smaller the bend radius can be, hence saving on valuable real-estate area on the silicon wafer.
- This is just one of the reasons why there is currently a trend towards smaller photonic circuit dimensions.